PHYSICAL REVIEW A, VOLUME 65, 051803(R)

Experimental coherent control of lasers

R. Gordon,[1,*] A. P. Heberle,[2] A. J. Ramsay,[1] and J. R. A. Cleaver[1]
[1]*Microelectronics Research Centre, Cavendish Laboratory, Cambridge, CB3 0HE, United Kingdom*
[2]*Hitachi Cambridge Research Laboratory, Cambridge, CB3 0HE, United Kingdom*
(Received 20 November 2001; published 8 May 2002)

We experimentally demonstrate coherent control of a laser. A resonant 100-fs optical pulse is injected into a vertical cavity surface emitting laser to introduce a field component with well-defined phase and thereby excite beating oscillations between the transverse lasing modes. By changing the relative phase between two injected pulses, we can enhance or destroy the beating oscillations and select which lasing modes are excited. We discuss resonant pulse injection into lasers and show how mode competition improves controllability by suppressing the phase-sensitive effects of the carriers.

DOI: 10.1103/PhysRevA.65.051803 PACS number(s): 42.55.Px, 42.79.Ta, 42.50.Ar

Coherent control of light-matter interaction has been a subject of significant interest to a broad range of disciplines [1–4] over recent years since the utilization of phase adds an additional degree of freedom. Using two or more time-separated light pulses with well-defined relative phase has been applied to the control of tetrahertz radiation [2], coherently coupled systems [3], and for the annihilation of excitons [4]. One key advantage of coherent control is that it allows for switching between states on time scales much shorter than the intrinsic relaxation [4].

All-optical switching [4], logic [5], and memories [6] are a few examples where coherent control may offer substantial speed improvements over traditional methods. It was quickly realized that the picosecond decoherence times in semiconductors (even at 4 K temperatures) were too short for any practical device application [7]. Stimulated emission is able to counteract coherence decay, but femtosecond coherent control of an active optical system, such as a laser, has until now never been demonstrated. Pulse injection in lasers biased above threshold has always been investigated in regimes where phase does not play a role [5,8–11], with single pulses or at wavelengths well away from the lasing transition.

In this paper, we experimentally demonstrate femtosecond coherent control of a laser. The model system used is a vertical cavity surface emitting laser (VCSEL) that provides the benefit of a single longitudinal mode $3\lambda/2$ microcavity resonator, and so propagation effects, which would be important in an edge-emitting laser [10], are not present. We show that injecting a pulse resonant with the VCSEL produces beating between the lasing transverse modes. Previous works have shown that injecting intense nonresonant pulses can set the *relative* phase between modes to produce mode beating [11]. By contrast, we show that injecting resonant pulses can influence the *absolute* phase of the modes. This is confirmed by phase-sensitive control of the mode beating with the injection of a second resonant pulse. We use the phase-sensitive control as an experimental tool to selectively excite specific oscillating modes. We discuss resonant pulse injection and show that mode competition can suppress the effects of the nonlinear carrier response that would otherwise be detrimental to coherent control.

The VCSEL's investigated were multimode commercial devices lasing at 855 nm and having a 3.5-mA threshold current. Resonant 100-fs optical pulses from a mode-locked Ti:sapphire laser (1 to 10 pJ per pulse, 855-nm center wavelength, and 82-MHz repetition rate) were focused onto the VCSEL with a 5-μm spot size. With this resolution, each pulse coupled into approximately 10 (lasing and nonlasing) transverse modes. A 7.5 μm-radius window in the top contact restricted pulse injection to within the concentric 10 μm radius active region defined by ion implantation. The VCSEL emission was up converted in a nonlinear crystal by sum-frequency generation with a time-delayed sampling pulse and detected with a photomultiplier tube. The delay of the sampling pulse was varied to obtain subpicosecond time resolution of the laser emission [10]. The injected and sampling pulses were polarized at 45° to the main polarization axis of the VCSEL to excite and detect both polarization senses.

Figure 1(a) shows the time-resolved VCSEL emission, spatially integrated in the far field, after the injection of a single optical pulse for two different bias currents. The inset to Fig. 1(a) shows a schematic of the experimental setup. The initial spike at time zero corresponds to reflection of the pulse from the VCSEL Bragg mirror. The increase in lasing emission after this first spike shows how much light enters the cavity. Due to the high reflectivity of the VCSEL mirror, approximately 0.5% of the injected optical pulse energy couples into the active region. In this experiment between 5 and 50 fJ of pulse energy is coupled into the cavity (divided up between the modes), which is three orders of magnitude smaller than that has been used previously for nonresonant pulse injection to excite mode oscillations in VCSEL's [11]. The energy of lasing light within the cavity is approximately 20 fJ at 12.5 mA.

The VCSEL emission shows oscillations resulting from the beating between transverse modes. The peak-to-peak magnitude of oscillation is 30% of the VCSEL's output power for the most intense injected pulses used. The intensity of beating varies linearly with injected optical pulse power. The percentage beating is ultimately limited by the spatial overlap between the transverse modes (as seen at the

*Email address: rg237@cam.ac.uk

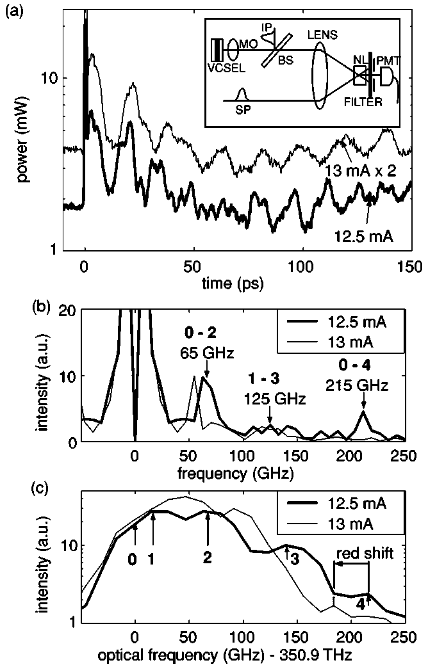

FIG. 1. (a) VCSEL emission after single 100-fs resonant optical pulse injection (at 0 ps) for 12.5-mA (thick line) and 13-mA (thin line) current injection. Inset shows experimental setup (MO denotes microscope objective, NL denotes β-BBO crystal, BS denotes beam splitter, PMT denotes photomultiplier tube, IP denotes injected pulse, and SP denotes sampling pulse). (b) Fourier transform of (a). Strong 65- and 215-GHz beat peaks for 12.5-mA current injection and 50-GHz beat peak for 13 mA. (c) Optical spectrum of free-running VCSEL at 12.5 mA and 13 mA. Lasing modes are labeled 0 to 4 for the 12.5-mA current.

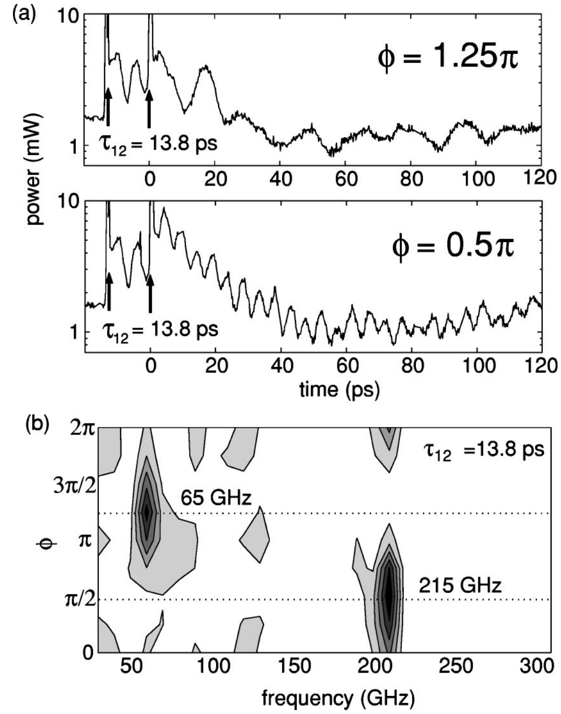

FIG. 2. (a) VCSEL emission at 12.5 mA after injection of two resonant optical pulses separated by $\tau_{12} = 13.8$ ps for two values of the relative phase between pulses, ϕ. Arrows indicate the times of pulse injection. (b) Contour plot of Fourier transform of VCSEL's response under same conditions as (a) over full cycle of ϕ.

detector) and the cw emission from nonexcited modes. The beating occurs at a series of frequencies between 50 and 215 GHz. The beat frequencies emitted vary with the bias current. In addition to the mode beating, weak relaxation oscillations with a 150-ps period are seen.

Figure 1(b) shows the Fourier transform of the curves in Fig. 1(a). Figure 1(c) shows the lasing spectrum of the VCSEL measured with a 0.46-m spectrometer. The VCSEL's lasing modes experience a 40-GHz redshift due to injection heating when the current is raised from 12.5 to 13 mA. In Fig. 1(c), the modes are labeled 0 through 4 at 0, 15, 65, 140, and 215 GHz (determined by fitting to Gaussian peaks with the spectrometer resolution full with at half maximum of 30 GHz). Modes 0 and 2 are orthogonally polarized to modes 1, 3, and 4 (not shown).

The injected pulse creates beating oscillations between transverse lasing modes. The beat peak resonances at 65 and 215 GHz in Fig. 1(b) agree well with the spacing between the free-running (i.e., without pulse injection) laser modes 0–2 and 0–4 in Fig. 1(c). There is also a small 125-GHz beat peak corresponding to the spacing between modes 1 and 3.

In Ref. [11], it was shown that nonresonant injection adds carriers to the inverted gain medium by absorption, which increases the gain and excites new lasing modes. By contrast, the resonant pulse injection used here removes carriers by stimulated emission that reduces the gain and so the emergence of new lasing modes is not expected. At 12.7 mA, there is a change in the free-running lasing spectrum where mode zero disappears and the spectral width becomes narrower. Simultaneously, the 65 GHz and 215-GHz beat components disappear and a 50-GHz beat peak emerges [see Fig. 1(b)]. Similar observations have been made for other current values and on other VCSEL's, all confirming that the free-running lasing modes produce the observed beating. This observation is key to the control experiments that follow, because it shows that we can resonantly interact with the preexistent lasing modes without introducing new ones.

Figure 2(a) shows the response of the VCSEL's emission to double pulse injection. The pulse pair is created by a Michelson interferometer actively stabilized to better than 0.06 fs variance in pulse separation, τ_{12}. We control the response of the VCSEL by varying the relative phase ϕ between the pulses with subwavelength changes to the pulse separation. The VCSEL emission shows 65-GHz and 215-GHz oscillation for $\phi = 1.25\pi$ and 0.5π, respectively. We have observed a phase-sensitive response of the laser to the second injected pulse up to a maximum 175-ps separation (limited by the setup) between the two injected pulses. This time separation is significantly longer than the photon cavity lifetime (2 ps), but less than the VCSEL coherence time (>1 ns).

Figure 2(b) shows the power spectrum of the VCSEL's output after double pulse injection for an entire cycle of relative phase between the two injected pulses. It is possible to tune the emission to different isolated oscillation frequencies

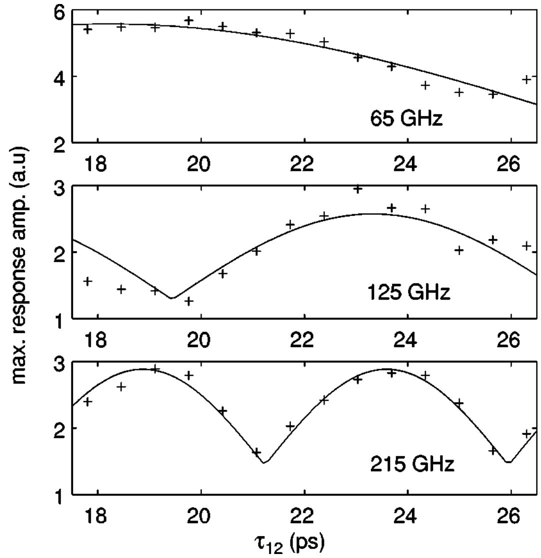

FIG. 3. Crosses show measured maximum of VCSEL response (at frequencies of 65 GHz, 125 GHz, and 215 GHz) to two injected optical pulses with varying separation τ_{12}. The solid curve shows a $1+|\cos(\Omega\tau_{12}/2)|$ fit.

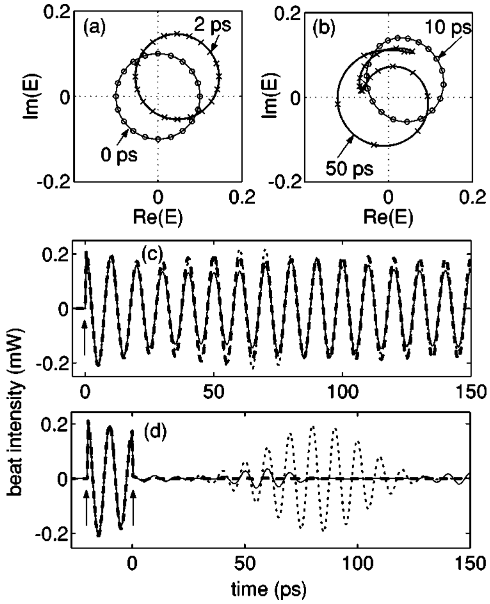

FIG. 4. Complex field of isolated single mode ($\beta_{jj}=1$) for injection of 100-fs resonant pulse with $\theta=\pi/4$, at times (a) $\leqslant 0$ ps and 2 ps, and (b) 10 ps and 50 ps. Beating component between two modes after resonant pulse injection (times indicated with arrows) for (c) single pulse, and (d) double pulse annihilation control for $\beta_{jj}=1$ (dotted line), $\beta_{jj}=0.5$ (solid line), and three mode case (dashed line).

by adjusting ϕ. In this manner, we can select which modes are excited by coherent control. In Fig. 2(a) bottom, for example, we selectively excite the two weakest lasing modes to beat for over 120 ps without exciting the other oscillating modes.

Figure 3 shows the experimental maximum (over all phase values, ϕ) Fourier transform amplitude at each beat frequency separation between the two injected pulses. It may be shown that the maximum coherent enhancement for impulsive excitement of two linear oscillators with frequency difference Ω may be written as $1+|\cos(\Omega\tau_{12}/2)|$. A fit of the observed maximum beat amplitude to this expression is shown in Fig. 3. The beat frequencies obtained by fitting were 55, 128, and 220 GHz, respectively. These values are in good agreement with the actual beat frequencies shown in Fig. 1 (a). How can this linear control behavior exist in an active laser system, in spite of the nonlinear coupling between the carriers and the optical field?

To understand some of the observed features of resonant pulse injection and coherent control, we analyze the commonly used laser rate equations in dimensionless form, for the simplified case of two modes, phenomenologically including the effect of mode competition,

$$\dot{E}_j(t)=\frac{1+i\alpha}{2}\sum_k \beta_{jk}N_k(t)E_j(t)+i\omega_j E_j(t)+\kappa_j E_{\rm in}(t), \tag{1}$$

$$\dot{N}_j(t)=P_j-\gamma N_j(t)-[N_j(t)+1]\sum_k \beta_{jk}|E_k(t)|^2, \tag{2}$$

where $E_j(t)$ and $N_j(t)$ are the complex electric field and real carrier density of mode $j,k=1,2$, P_j is the carrier injection term, β_{jk} quantifies the overlap of mode k with $N_j(t)$ (with $\Sigma_k\beta_{jk}=1$), $\gamma=0.002$ is the carrier lifetime, ω_j is the angular frequency, $\alpha=2.5$ is the linewidth enhancement factor, κ_j is the in-coupling rate of the injected field, $E_{\rm in}(t)=A_{\rm in}(t)\exp[i\theta(t)]$, with $A_{\rm in}(t)$ real. Time is measured in units of the cavity lifetime. $\beta_{jj}=1$ describes two independent laser modes, whereas $\beta_{jj}=0.5$ describes two coupled modes equally sharing the carriers (e.g., carrier diffusion is large or modal overlap is uniform). Intensity beating is neglected from Eq. (2) since the beat period is an order of magnitude shorter than the overall relaxation time.

The stable steady-state lasing solutions give $N_j=0,|E_j|^2=P_j$ for $\beta_{jj}=1$, and $\Sigma_j|E_j|^2=\Sigma_jP_j$ for $\beta_{jj}=0.5$. We start with the laser operating at steady state and inject a pulse with $\theta(t)$ equal to zero around the time zero and ϕ around time τ_{12}. The injected pulse energy is 40% the total energy for each mode.

Figures 4(a) and 4(b) show the electric field of a single laser mode [described by Eqs. (1) and (2), $\beta_{jj}=1$ in the rotating frame $\omega_j=0$] for different times after the injection of a single resonant pulse. We show the electric-field vector for an ensemble of such excitations, with randomly distributed initial phase of the VCSEL, thereby mapping out a circle in the complex plane for times $\leqslant 0$ ps. The injected pulse translates this circle in the direction given by θ ($\pi/4$ shown), which causes the ensemble average phase to equal θ. Therefore the injected pulse can provide a type of *phase locking*.

The carriers provide an instantaneous frequency shift [through α in Eq. (1)] that does little to influence the phase of the mode for times comparable to the cavity lifetime (2 ps), because the carrier change is relatively small. Figure 4(b) shows that 50 ps after the injected pulse, the frequency shift is substantial and the carrier induced phase shift builds up to distort the phase distribution. Injecting light into the short-lived nonlasing modes leads to a similar phase shift through the carriers, but this uniform phase shift is independent of the phase of the lasing modes and will not produce beating.

When we average over all phases, as in the experiment, and consider two lasing modes, the phase locking provided by the injected pulse produces beating. Fig. 4(c) shows this beat component for two modes after the injection of a single resonant pulse, for different values of β_{jj}.

To perform control of the beating, we inject a second pulse out of phase with the first (angle π change to θ). This returns the translated circle in Figure 4(a) back to the origin. More generally, when the carrier effects are negligible ($N_k=0$) and within the rotating frame ($\omega_j=0$), we see from Eq. (1) that if the integral over the injected field is zero, then the mode will return to its unperturbed configuration.

Whereas varying the carrier coupling (β_{jj}) produces only minor effects for single pulse injection, pronounced qualitative differences exist for double pulse injection. Figure 4(d) shows coherent annihilation of the beating for the two extremes of β_{jj} (0.5 and 1), with arrows indicating the times of injected pulses. For $\beta_{jj}=1$, the beating oscillations have a strong reemergence after 50 ps that is predominantly due to a carrier induced relative phase shift between the in-phase and out-of-phase injection. We have not observed this phenomenon in our experiments, so each mode cannot be treated as an isolated laser.

For $\beta_{jj}=0.5$, the carriers do not introduce a relative phase shift between the modes (since the modes share the carriers equally), and the reemergent oscillations are suppressed. Therefore sharing of the carriers from modal overlap actually reduces the nonlinear relative phase shift between the modes that can be detrimental to control. A small reemergent oscillation persists due to the phase-sensitive amplitude change with pulse injection.

The dashed line in Figure 4(d) shows suppression of all oscillations after the control pulse when a third mode is added (with no pulse injection, four times as intense as the other modes and all modes coupled equally to the carriers). Adding this intense mode reduces the perturbation of the injected pulse relative to the total intensity of the laser. As a consequence, the amplitude relaxation is clamped and we have near perfect linear control.

In conclusion, we have demonstrated ultrafast coherent control of a laser by injecting two optical pulses resonant with the laser. The experiments also demonstrate that coherent control can be used as an ultrafast experimental tool to selectively probe specific oscillators in a coupled oscillator system. We have shown how resonant injection produces mode beating through direct field injection into the lasing modes. We have also discussed how mode competition improves the ability to perform coherent control. The >1 ns coherence time of lasers may be applied to room-temperature coherent optical switching, memory and logic devices.

[1] P. Brumer and M. Shapiro, Chem. Phys. Lett. **126**, 541 (1986).
[2] P.C.M. Planken *et al.*, Phys. Rev. B **48**, 4903 (1993).
[3] S. Osnaghi *et al.*, Phys. Rev. Lett. **87**, 037902 (2001).
[4] A.P. Heberle, J.J. Baumberg, and K. Köhler, Phys. Rev. Lett. **75**, 2598 (1995).
[5] F. Prati, M. Travagnin, and L.A. Lugiato, Phys. Rev. A **55**, 690 (1997).
[6] M. Brambilla *et al.*, Phys. Rev. Lett. **79**, 2042 (1997).
[7] D.S. Citrin, Phys. Rev. Lett. **77**, 4596 (1996).
[8] A. Klehr and R. Müller, J. Appl. Phys. **81**, 2064 (1997).
[9] S.G. Hense and M. Wegener, Appl. Phys. Lett. **74**, 920 (1999).
[10] M. Kauer *et al.*, Appl. Phys. Lett. **72**, 1626 (1998).
[11] O. Buccafusca *et al.*, Appl. Phys. Lett. **67**, 185 (1995).